International Scholarly Research Network
ISRN Optics
Volume 2012, Article ID 476817, 12 pages
doi:10.5402/2012/476817

Research Article

Quantum Dynamics of Interacting Modes in Intracavity Third Harmonic Generation Process

Menua Gevorgyan[1] and Saribek Gevorgyan[2]

[1] *Moscow Institute of Physics and Technology, Moscow, Russia*
[2] *Institute for Physical Research, National Academy of Sciences of Armenia, Ashtarak, Armenia*

Correspondence should be addressed to Saribek Gevorgyan, saribek@ipr.sci.am

Received 6 September 2012; Accepted 17 October 2012

Academic Editors: M. Goksör, Y. S. Kivshar, M. Midrio, and D. H. Woo

We study the quantum dynamics of the number of photons of the interacting modes, the dynamics of the quantum entropy, and the Wigner function of the states of the fundamental and the third harmonic modes for the process of intracavity third harmonic generation. It is shown that the quantum dynamics of the system strongly depends on the external resonant perturbation of the fundamental mode and on the coupling coefficient of the interacting modes. In the region of long interaction times, the modes of the field can be both in stable and in unstable states—depending on the above-mentioned quantities. In the paper, we also investigate the dynamics of transition of the system from stable to unstable states.

1. Introduction

For certain optical processes, such as the intracavity generation of the second and third harmonics [1–3], stationary solutions for the dynamics of the number of photons are stable only for relatively small pump amplitudes. For these systems, a certain critical value of the pump field exists above which small fluctuations in the system do not decay, and the dynamics of the semiclassical value of the photon number changes to the regime of self-oscillations. Among the unstable optical systems mentioned above, the intracavity second harmonic generation (SHG) is rather well investigated. Studies [1, 2, 4–10] are devoted to the investigation of the behavior of the intracavity SHG above the bifurcation point of the optical system. As compared to the case of the SHG, the unstable behaviour of intracavity third harmonic generation (THG) is insufficiently studied. In [3], the Langevin equations for stochastic field amplitudes for the THG process were derived in the positive P-representation. The bifurcation point of the system was found, and it was shown that, above this point, the dynamics of the number of photons of the interacting modes changes to the regime of self-oscillations. Then, in [11], the distribution functions for the phases of the fundamental mode and of the third harmonic mode above the bifurcation point of the system were studied in the positive P-representation. The distribution functions were shown to have a two-component structure. In addition to this, the functions of joint distribution of the number of photons and phases of the interacting modes were studied. In [12], the distribution functions of the number of photons of the fundamental and the third harmonic modes above the bifurcation point of the system, as well as the joint distribution function of the number of photons of the interacting modes, were studied in the positive P-representation. It is shown that, when the system turns from stable to the unstable region, the above-mentioned functions change from one-component structure to two-component structure.

In the present paper, we study the quantum dynamics of the number of photons and the dynamics of quantum entropy and the Wigner functions of the fundamental and third harmonic modes for the process of intracavity third harmonic generation. The dependence of the state of the field upon the coupling coefficient and upon the amplitude of the external perturbing field acting on the fundamental mode is studied. We also investigate the quantum dynamics of the transition of the system from stable state to unstable state.

2. The Nonlinear System and the Basic Equations

Consider a model of THG inside a two-mode cavity. A nonlinear medium is placed inside a cavity tuned to the frequencies of the fundamental mode ω_1 and of the third harmonic ω_2, where $\omega_2 = 3\omega_1$. The fundamental mode is resonantly perturbed by an external classical field. The density matrix equation, which describes this optical system, can be written in the following form:

$$\frac{\partial \rho}{\partial t} = (i\hbar)^{-1}\left[H_{\text{sys}}, \rho\right] + L(\rho), \tag{1}$$

where

$$H_{\text{sys}} = \frac{i\hbar\chi}{2}\left(a_1^{+3}a_2 - a_1^3 a_2^+\right) + i\hbar E\left(a_1^+ - a_1\right), \tag{2}$$

$$L(\rho) = \sum_{i=1}^{2}\frac{\gamma_i}{2}\left(2a_i\rho a_i^+ - \rho a_i^+ a_i - a_i^+ a_i \rho\right). \tag{3}$$

Here, a_i and a_i^+ $(i = 1, 2)$ are the annihilation and creation operators of photons of the fundamental mode and the third harmonic mode, respectively; χ is the coupling coefficient of the modes, which is proportional to the nonlinear susceptibility $\chi^{(3)}$ of the medium; E is the classical amplitude of the perturbing field at the frequency ω_1; γ_i $(i = 1, 2)$ are the damping coefficients of the interacting modes. In (2) phase of the perturbing field is omitted for simplicity.

In order to investigate the quantum dynamics of the optical system, we calculate the mean number of photons of the modes

$$n_i(t) = Tr\left(\rho_i(t) a_i^+ a_i\right), \quad (i = 1, 2), \tag{4}$$

where the density matrices of the interacting modes are obtained by calculating the trace of the density matrix of the system

$$\rho_{1(2)} = Tr_{2(1)}(\rho). \tag{5}$$

We also consider the dynamics of the quantum entropy of the modes of the field

$$S_i(t) = -Tr\left(\rho_i(t)\ln\rho_i(t)\right), \quad (i = 1, 2). \tag{6}$$

We calculate the quantum entropy of the modes of the field by the numerical diagonalization of the corresponding density matrices in the Fock basis [13]. In order to study quantum properties of the optical systems, we also calculate the Wigner function of the states of the modes of the field. These functions are calculated in polar coordinates $x = r\cos(\theta)$, $y = r\sin(\theta)$ by using formula in [13]:

$$W_i(r, \theta) = \sum_{m,n}\rho_{i,mn} w_{mn}(r, \theta), \quad (i = 1, 2). \tag{7}$$

Here, $\rho_{i,mn}$ are the matrix elements of the density matrices of the interacting modes in the Fock basis. The expression for $w_{mn}(r, \theta)$ is defined by the formula

$$w_{mn}(r, \theta) = \begin{cases} \dfrac{2}{\pi}(-1)^n\left(\dfrac{n!}{m!}\right)^{1/2}\exp(i(m-n)\theta)\exp\left(-2r^2\right)(2r)^{m-n}L_n^{m-n}\left(4r^2\right), & m \geq n, \\ \dfrac{2}{\pi}(-1)^m\left(\dfrac{m!}{n!}\right)^{1/2}\exp(i(m-n)\theta)\exp\left(-2r^2\right)(2r)^{n-m}L_m^{n-m}\left(4r^2\right), & m \geq n. \end{cases} \tag{8}$$

Here, L_p^q are the Laguerre polynomials.

Equation (1) for the density matrix of the optical system is solved applying the numerical Monte Carlo wavefunction method [14]. In this method, the density matrix of the system is represented as the expectation for the density matrices of the quantum trajectories; each of which represents a pure state, which can be found by using certain algorithm:

$$\begin{aligned} \rho(t) &= M\left\{\left|\phi^{(\alpha)}(t)\right\rangle\left\langle\phi^{(\alpha)}(t)\right|\right\} \\ &= \lim_{N\to\infty}\frac{1}{N}\sum_{(\alpha)}^{N}\left|\phi^{(\alpha)}(t)\right\rangle\left\langle\phi^{(\alpha)}(t)\right|. \end{aligned} \tag{9}$$

Here, (α) is the trajectory number; N is the number of all independent quantum trajectories.

The algorithm to calculate one quantum trajectory of the system is similar to the corresponding algorithm for the process of intracavity second harmonic generation, which is presented in [10].

We investigate the dynamics of the system using dimensionless time $\tau = \gamma_1 t$ and dimensionless parameters

$$\varepsilon = \frac{E}{\gamma_1}, \qquad r = \frac{\gamma_2}{\gamma_1}, \qquad k = \frac{\chi}{\gamma_1} \tag{10}$$

for the ratio of dumping coefficients of the modes $(r = 1)$ in the case of evolution of the system from initial vacuum state. The mean number of photons, the quantum entropy, and the Wigner functions of the modes are calculated using 1000 independent quantum trajectories of the optical systems.

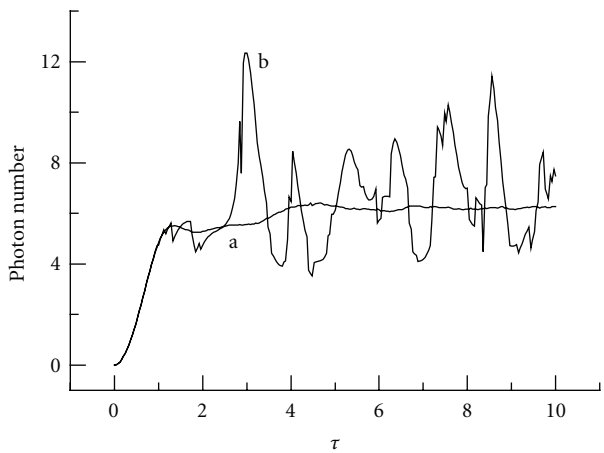

Figure 1: Dynamics of the mean number of photons (curve a) and of the number of photons of an arbitrarily chosen quantum trajectory (curve b) of the fundamental mode, for the values of the system parameters $\varepsilon = 3$, $k = 0.3$.

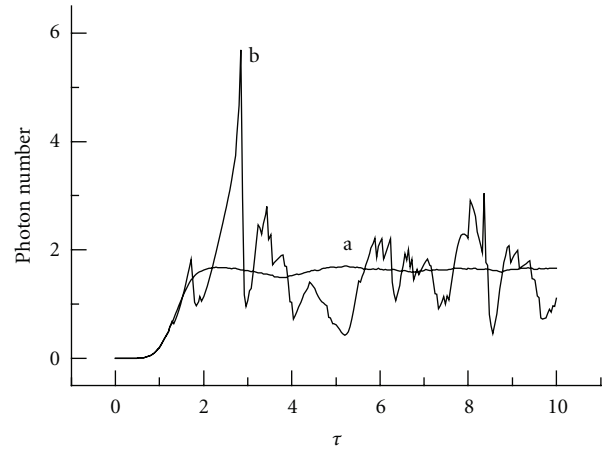

Figure 2: Dynamics of the mean number of photons (curve a) and the number of photons of an arbitrarily chosen quantum trajectory (curve b) of the third harmonic mode, $\varepsilon = 3$, $k = 0.3$.

3. The Quantum Dynamics of the System in the Case of Strong Coupling of the Modes and Strong Perturbation of the Fundamental Mode

Studied in this section is the quantum dynamics of the interacting modes of the optical system in the region of strong coupling of the modes ($k = 0.3$) and in the case of a strong external perturbation of the fundamental mode ($\varepsilon = 3$).

Figure 1 shows the quantum dynamics of the number of the photons of the fundamental mode (curve a) and the dynamics of the number of photons of the same mode for an arbitrarily chosen quantum trajectory of the optical system (curve b). In the region of long interaction time, the dynamics of the number of photons of a single trajectory differs much from the dynamics of the mean number of photons of the mode. The latter observation shows that there are strong fluctuations in the number of photons of the fundamental mode in the region of long interaction times ($\tau > 1$). In the region of short interaction time ($\tau < 1$), the dynamics of the mean number of photons of the mode is the same as the dynamics of the number of photons of an arbitrarily chosen quantum trajectory. For long interaction times, small fluctuations in the number of photons do not decay, which leads to a significant difference between the dynamics of the mean number of photons and the dynamics of the photon number of an arbitrarily chosen quantum trajectory.

Figure 2 shows the quantum dynamics of the number of the photons of the third harmonic mode (curve a) and the dynamics of the number of photons of an arbitrarily chosen quantum trajectory of the same mode (curve b). As in the case of the fundamental mode, in the region of short interaction times ($\tau < 1$), the dynamics of the number of photons of a single quantum trajectory is the same as the dynamics of the mean number of photons, and in the region of large interaction times ($\tau > 1$), the number of photons of a single quantum trajectory strongly fluctuates around the mean number of photons of the mode. The latter observation shows that the system turns to region of unstable behaviour, where small fluctuations of the number of photons of the interacting modes do not damp.

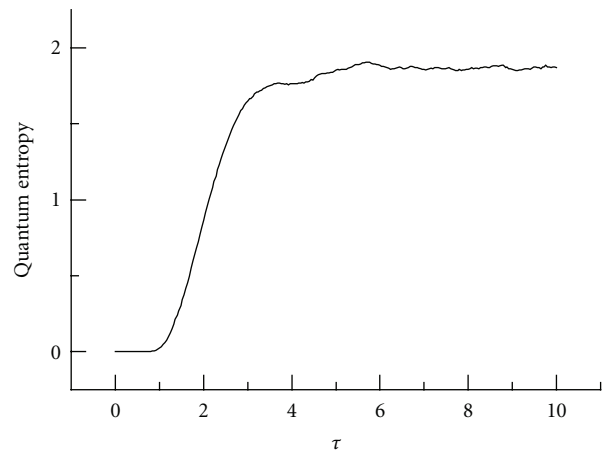

Figure 3: Dynamics of the quantum entropy of the fundamental mode for values of the system parameters $\varepsilon = 3$, $k = 0.3$.

Figure 3 shows the dynamics of the quantum entropy (6) of the fundamental mode. In the region of short interaction times, the quantum entropy of the mode is equal to zero, which indicates that in this region of interaction the mode is in a pure state and the ensemble of the quantum trajectories consists of a single term. The latter observation explains the coincidence of the dynamics of the number of photons of a single quantum trajectory and of the dynamics of mean number of photons (see Figure 1). After that, the quantum entropy of the mode starts to grow. Then, in the region of long interaction times ($\tau > 4$), it obtains a stationary value. In this region of interaction times, the state of the

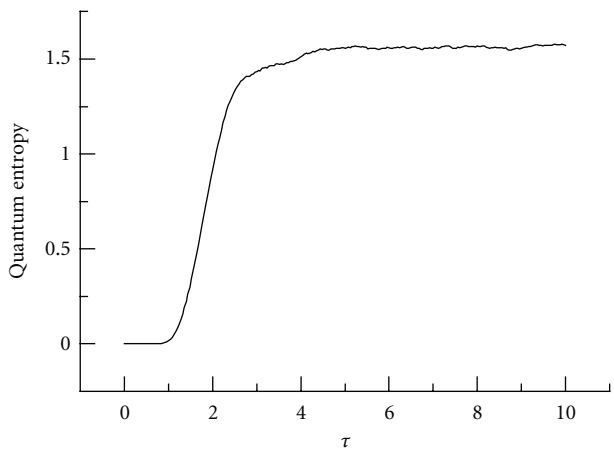

Figure 4: Dynamics of the quantum entropy of the third harmonic mode for the values of the system parameters $\varepsilon = 3$, $k = 0.3$.

system almost does not change any more and it represents a statistical mixture of pure states.

Figure 4 shows the dynamics of the quantum entropy of the third harmonic mode. As in the case of the fundamental mode, the quantum entropy of the third harmonic mode is equal to zero in the region of small interaction times. The mode is in a pure state and the ensemble of the quantum trajectories consists of a single term, which explains the coincidence of the dynamics of the number of photons of a single quantum trajectory and the dynamics of the mean number of photons in the region of small interaction times (see Figure 2). Then, the quantum entropy of the mode starts growing, and, in the region of the long interaction times ($\tau > 4$), it turns to stationary value. After that, the state of the system remains almost unchanged. The stationary value of the quantum entropy of the third harmonic is less than the stationary value of quantum entropy of the fundamental mode (see Figures 3 and 4).

Shown in Figure 5 is the dynamics of the Wigner function of the state of the fundamental mode. Here, Figure 5(a) shows the Wigner function of the initial vacuum state. Figures 5(b), 5(c), 5(d), 5(e), and 5(f) show the Wigner function of the state of the fundamental mode at the times of interaction $\tau = 1$, $\tau = 1.5$, $\tau = 2$, $\tau = 3$, and $\tau = 10$, respectively. At time $\tau = 1$ the system is in a pure coherent state with zero quantum entropy, into which it changed from initial vacuum state. At that moment, the number of photons has already reached almost the maximum value and does not change further (see Figure 1). After that, there is a sharp growth in the quantum entropy. The latter observation shows that although the energy of the mode does not change, the state starts to change sharply. Near time $\tau = 1.5$ the mode has already changed from a coherent state to a squeezed state (see Figure 5(c)). In this state, the quantum entropy of the fundamental mode is approximately 0.3, which shows that the system is not in a pure state. After that, as the the quantum entropy increases, the squeezed state of the fundamental mode begins to decay gradually, and at time $\tau \approx 2$ (see Figure 5(d)), the system gradually changes from a stable state into an unstable state. At time $\tau \approx 3$, the quantum entropy of the mode already almost reaches the maximal value 1.7, (the stationary value of the quantum entropy of the mode is approximately 1.9), and the system changes to unstable state, the Wigner function of which is shown in Figure 5(e). After that, the quantum entropy of the fundamental mode changes to stationary value. The Wigner function of the stationary state of the fundamental mode at time $\tau = 10$ is shown in Figure 5(f). It only slightly differs from the Wigner function shown in Figure 5(e), and it represents the unstable stationary state of the fundamental mode, which has two-state components.

Shown in Figure 6 is the dynamics of the Wigner function of the state of the third harmonic mode. Figures 6(a), 6(b), 6(c), 6(d), and 6(e) show the Wigner function of the state of the third harmonic mode at the times of interaction of the modes of the optical system, $\tau = 1$, $\tau = 1.5$, $\tau = 2$, $\tau = 3$, and $\tau = 10$, respectively. The mode was changing from initial vacuum state into a pure coherent state with (Figure 6(a)) zero quantum entropy at time $\tau \approx 1$ (see Figure 4). Meanwhile, the number of photons of the mode (see Figure 2) grew insignificantly, and the coherent state of the system was close to vacuum state, which also reflects the Wigner function in Figure 6(a). After that the quantum entropy of the system starts to grow, and at time $\tau \approx 1.5$, it reaches the value 0.3. The Wigner function of the state of the mode at time $\tau = 1.5$ is shown in Figure 6(b). It represents a squeezed state with a slightly squeezed quadrature component. After that, as the quantum entropy of the system grows, the squeezed state of the system begins to decay. The Wigner function of the state of the mode at time $\tau = 2$ is shown in Figure 6(c). The quantum entropy of this state is approximately equal to 0.9. A stationary unstable state begins to form in the system, the Wigner function of which at time $\tau = 3$ is shown in Figure 6(d). The quantum entropy of this state is approximately equal to 1.5, and it has almost reached the stationary value. After that the state of the system almost does not change. The Wigner function of the state of the third harmonic mode for the region of long interaction time ($\tau = 10$) is shown in Figure 6(e). It has a cylindrical form, and it represents the state of the mode of the third harmonic with completely undefined phase. The system is in an unstable state with an undefined phase. The quantum entropy of the stationary state is approximately equal to 1.6.

Figures 7 and 8 represent the Wigner functions of two arbitrarily chosen quantum trajectories of the optical system in the region of long interaction time, $\tau = 10$. Figure 7(a) represents the Wigner function of the state of the fundamental mode, and Figure 7(b) represents the Wigner function of the state of the third harmonic mode of an arbitrarily chosen quantum trajectory. Figures 8(a) and 8(b) represent the Wigner functions of the states of the fundamental and the third harmonic modes of another arbitrarily chosen quantum trajectory, respectively. The Wigner functions of the corresponding modes of two different quantum trajectories differ much from each other. The latter explains the high values of the quantum entropy of the modes in this region of interaction times.

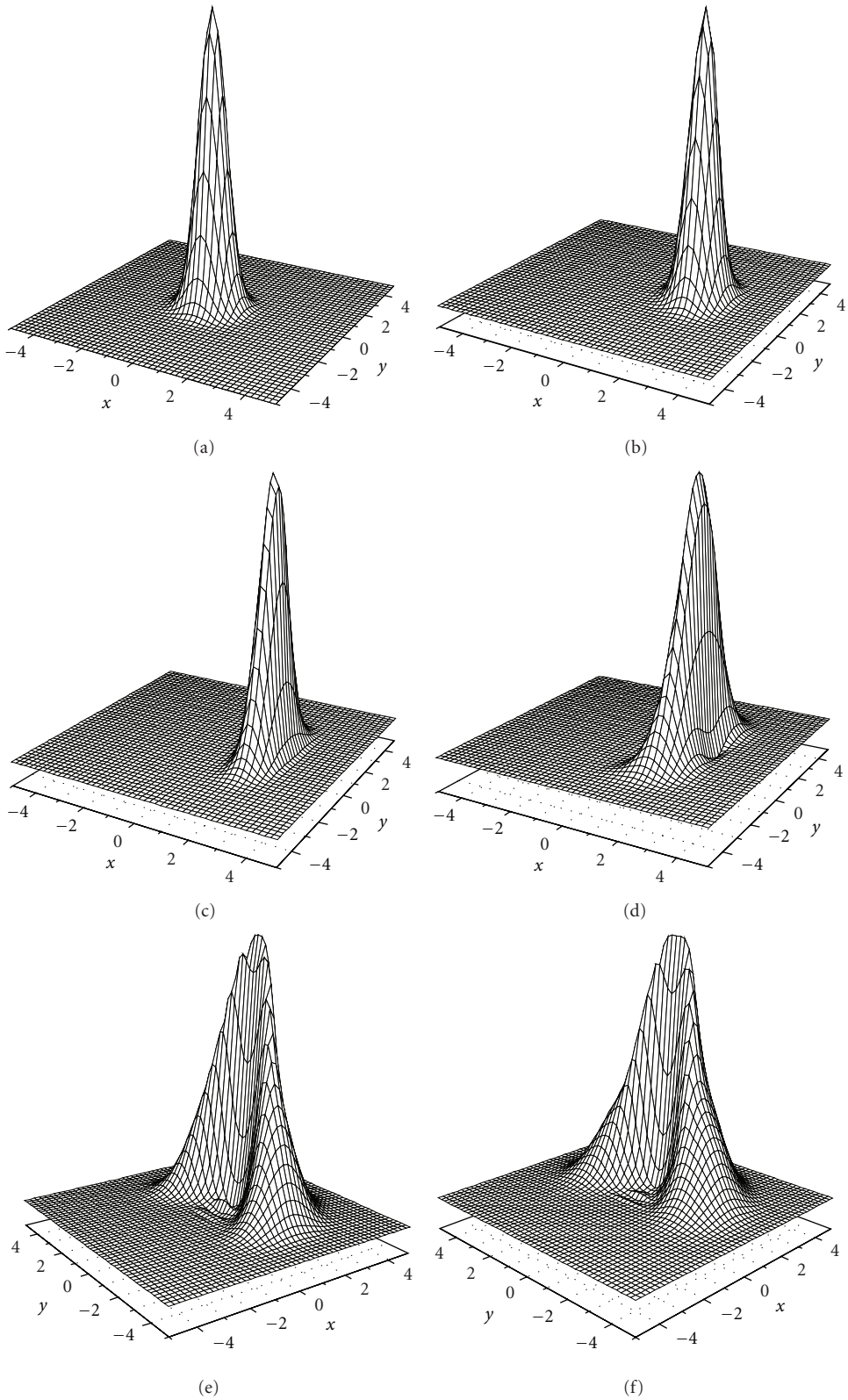

Figure 5: Dynamics of the Wigner function of the state of the fundamental mode for the values of the system parameters $\varepsilon = 3$, $k = 0.3$. Figures (b), (c), (d), (e), and (f) illustrate the Wigner functions of the fundamental mode at times of interaction of the modes $\tau = 1$, $\tau = 1.5$, $\tau = 2$, $\tau = 3$, and $\tau = 10$, respectively.

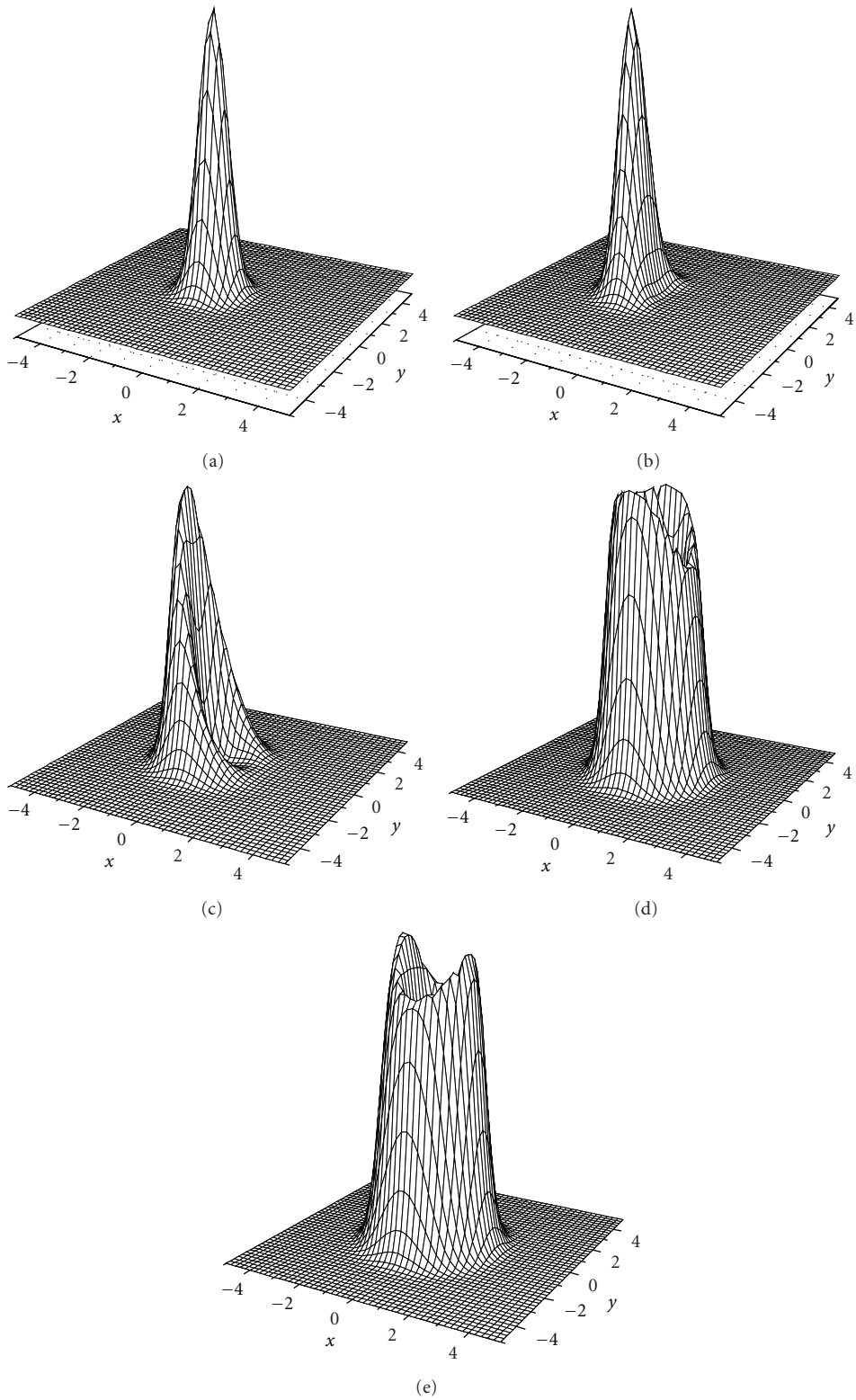

Figure 6: Dynamics of the Wigner function of the state of the third harmonic for the values of the system parameters $\varepsilon = 3$, $k = 0.3$. Figures (a), (b), (c), (d), and (e) illustrate the Wigner functions of the third harmonic mode at times of interaction $\tau = 1$, $\tau = 1.5$, $\tau = 2$, $\tau = 3$, and $\tau = 10$, respectively.

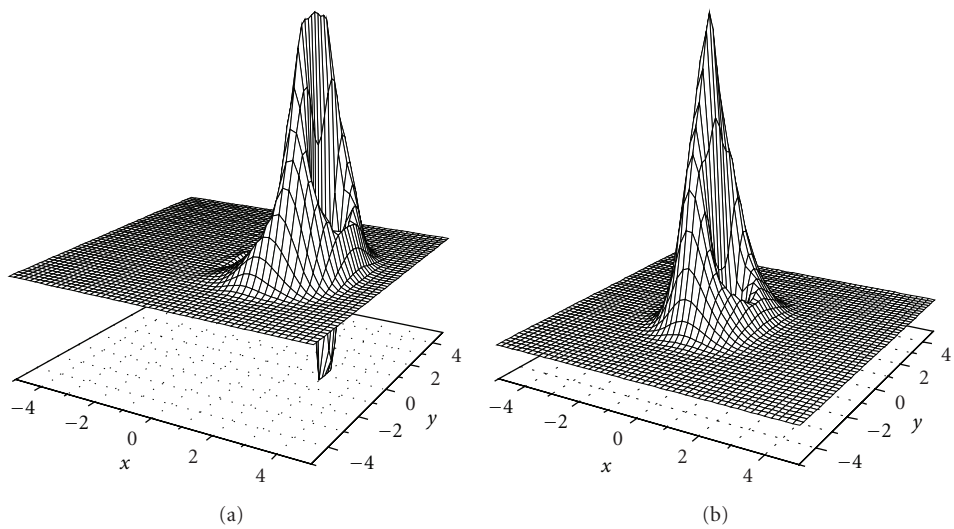

Figure 7: Wigner functions of the states of the fundamental mode (a) and the third harmonic mode (b) of an arbitrary quantum trajectory of the optical system in the region of long interaction times ($\tau = 10$) and for the values of the parameters of the system $\varepsilon = 3$, $k = 0.3$.

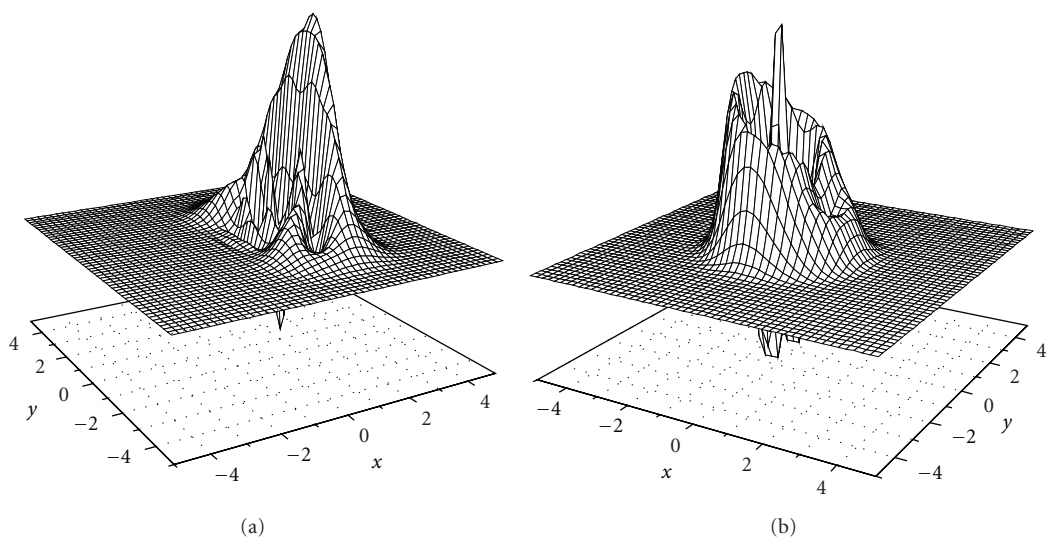

Figure 8: Wigner functions of the states of the fundamental mode (a) and the third harmonic mode (b) of an arbitrary quantum trajectory of the optical system in the region of long interaction times ($\tau = 10$) and for the values of the parameters of the system $\varepsilon = 3$, $k = 0.3$.

4. The Quantum Dynamics of the Interacting Modes in the Case of Strong Coupling of the Modes and Weak Perturbation of the Fundamental Mode

In this section, we study the quantum dynamics of the system in the case where perturbation of the fundamental mode is weak ($\varepsilon = 1$) as compared to the case studied in the previous section ($\varepsilon = 3$). The coupling coefficient remains the same ($k = 0.3$).

Figure 9 illustrates the quantum dynamics of the number of photons of the fundamental mode (curve a) and the dynamics of the number of photons of an arbitrarily chosen quantum trajectory (curve b). In the region of short interaction time ($\tau < 2$), the dynamics of the mean number of photons coincides with the dynamics of the number of photons of an arbitrarily chosen quantum trajectory of the fundamental mode. In the region of long interaction times, we explain the slight fluctuations of the number of photons of an arbitrarily chosen quantum trajectory of the system to be due to weak perturbation of the fundamental mode. The system is in stable state.

Figure 10 illustrates the quantum dynamics of the mean number of photons (curve a) and of the number of photons of an arbitrarily chosen trajectory (curve b) of the third harmonic. In the region of short interaction times ($\tau < 2$), the dynamics of the mean number of photons of the third harmonic coincides with the dynamics of the number of photons of an arbitrarily chosen quantum trajectory. In the region of long interaction times, we explain the large

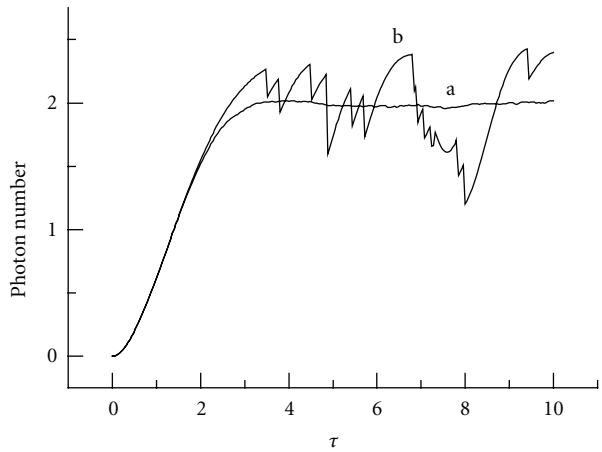

Figure 9: Dynamics of the mean number of photons (curve a) and of the number of photons of an arbitrary quantum trajectory of the fundamental mode for the values of the system parameters $\varepsilon = 1$, $k = 0.3$.

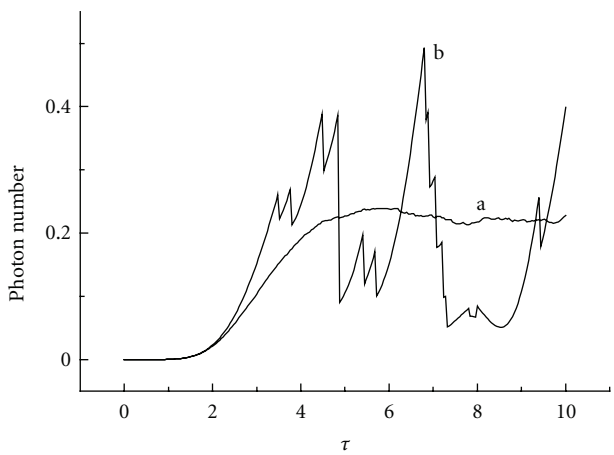

Figure 10: Dynamics of the mean number of photons (curve a) and of the number of photons of an arbitrary quantum trajectory of the third harmonic mode for the values of the system parameters $\varepsilon = 1$, $k = 0.3$.

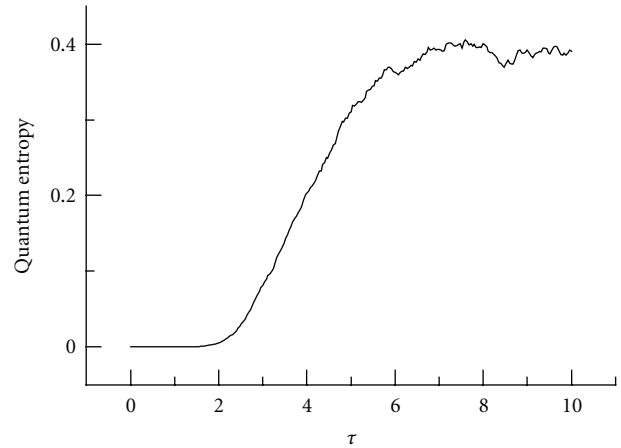

Figure 11: Dynamics of the quantum entropy of the fundamental mode for the values of the system parameters $\varepsilon = 1$, $k = 0.3$.

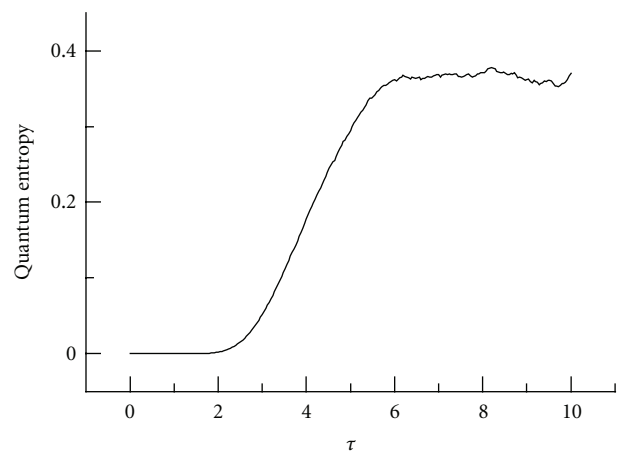

Figure 12: Dynamics of the quantum entropy of the third harmonic mode for the values of the system parameters $\varepsilon = 1$, $k = 0.3$.

fluctuations of the number of photons of an arbitrarily chosen trajectory around the mean number of photons to be due to small value of the number of photons.

Shown in Figures 11 and 12 is the dynamics of the quantum entropy of the fundamental and the third harmonic modes, respectively. In the region of short interaction time ($\tau < 2$), the quantum entropies of the modes are equal to zero, which shows that the modes are in pure states in this region of interaction times. Later, the quantum entropy of the modes starts growing. In the region of long interaction time ($\tau = 10$), it is approximately equal to 0.4. In contrast to the case of strong external perturbation of the fundamental mode, the stationary values of the quantum entropies of the modes are equal in the present case, and they are smaller than the corresponding values in the case of strong perturbation. That the values of quantum entropy are small shows that the ensemble of quantum trajectories consists of less terms in the present case than in the former one.

Shown in Figures 13 and 14 is the quantum dynamics of the Wigner function of the states of the fundamental and the third harmonic modes, respectively. Figures 13(a) and 14(a) represent the Wigner functions of the states of the fundamental and the third harmonic modes, respectively, at interaction time $\tau = 2$. Both of the functions represent a pure coherent state (the quantum entropy is equal to zero (see Figures 11 and 12)). At this time of interaction, the number of photons of the third harmonic (see Figure 10) is still small, and the Wigner function of the state of the mode represents a coherent state, which is close to vacuum state. Figures 13(b) and 14(b) represent the Wigner functions of the states of the fundamental and the third harmonic modes, respectively, in the region of long interaction times ($\tau = 10$). In the region of long interaction times, the fundamental mode changes from pure coherent state into squeezed stationary state, the value of quantum entropy of which equals 0.4. The mode of the third harmonic changes into a state, the Wigner function of

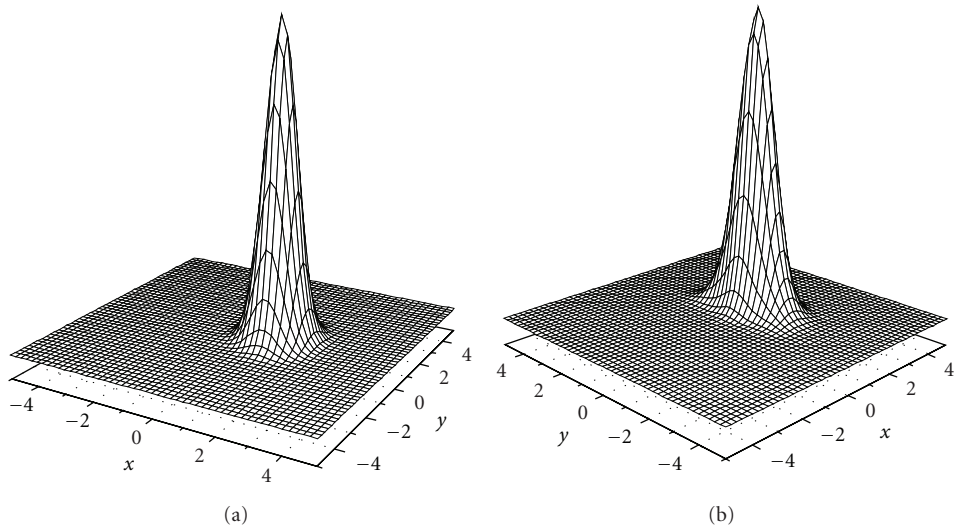

Figure 13: Dynamics of the Wigner function of the state of the fundamental mode for the values of the system parameters $\varepsilon = 1$, $k = 0.3$. Figures (a) and (b) illustrate the Wigner function at times of interaction of the modes $\tau = 2$ and $\tau = 10$, respectively.

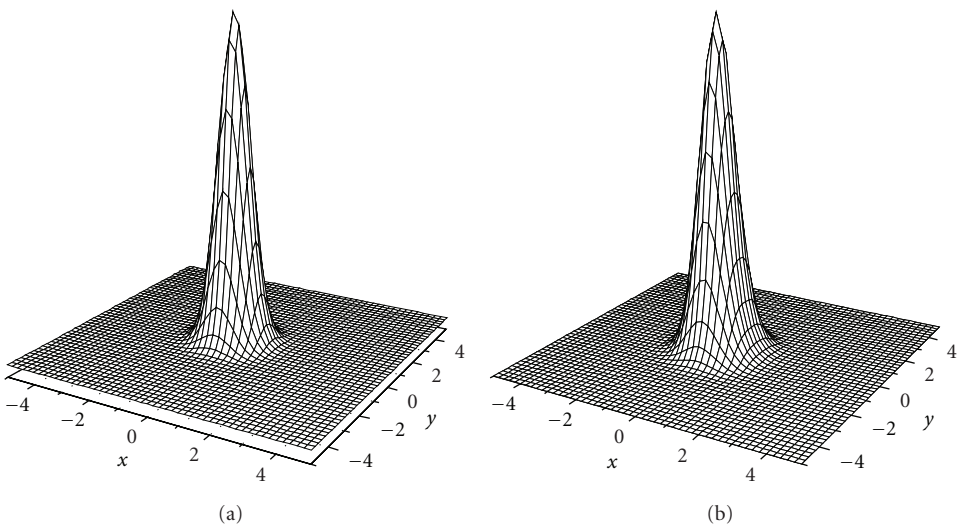

Figure 14: Dynamics of the Wigner function of the state of the third harmonic mode for the values of the system parameters $\varepsilon = 1$, $k = 0.3$. Figures (a) and (b) illustrate the Wigner function at times of interaction of the modes $\tau = 2$ and $\tau = 10$, respectively.

which is similar to the Wigner function of a coherent state, but the value of quantum entropy equals 0.4. The Wigner functions show that the system is in stable state in the region of long interaction times.

5. The Quantum Dynamics of the System in the Case of Weak Coupling of the Interacting Modes and Strong Perturbation of the Fundamental Mode

In this section, we investigate the quantum dynamics of the system in the case of weak coupling of the modes ($k = 0.1$) and strong external resonant perturbation ($\varepsilon = 3$) of the fundamental mode.

Shown in Figure 15 is the quantum dynamics of the number of photons of the fundamental mode (curve a) and of an arbitrarily chosen quantum trajectory of the fundamental mode (curve b). The dynamics of the number of photons and of an arbitrarily chosen quantum trajectory coincides in the region of short interaction times ($\tau < 2$). Later, the number of photons of an arbitrarily chosen quantum trajectory fluctuates around the mean number of photons of the fundamental mode. That the magnitude of the fluctuations is small, as compared to the magnitude of fluctuations of an arbitrarily chosen quantum trajectory shown in Figure 1, we explain to be due to weak coupling of the interacting modes.

Shown in Figure 16 is the quantum dynamics of the number of photons of the third harmonic mode (curve a)

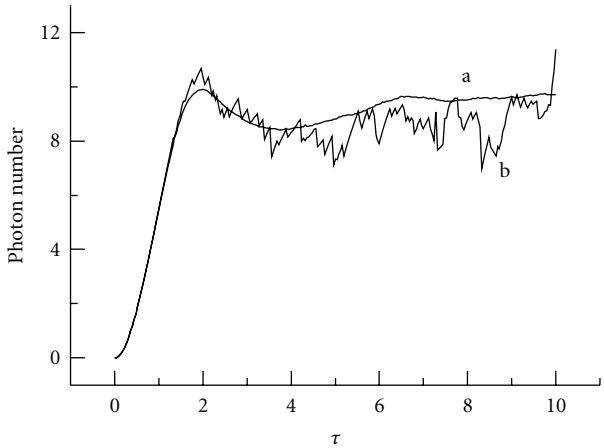

Figure 15: Dynamics of the mean number of photons (curve a) and of the number of photons of an arbitrary quantum trajectory (curve b) of the fundamental mode for the values of the system parameters $\varepsilon = 3$, $k = 0.1$.

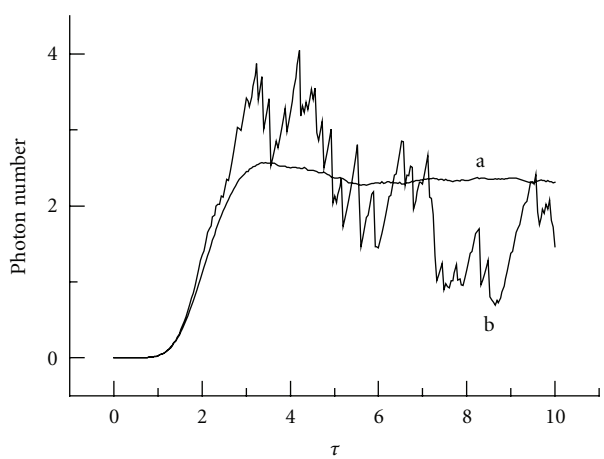

Figure 16: Dynamics of the mean number of photons (curve a) and of the number of photons of an arbitrary quantum trajectory (curve b) of the third harmonic mode for the values of the system parameters $\varepsilon = 3$, $k = 0.1$.

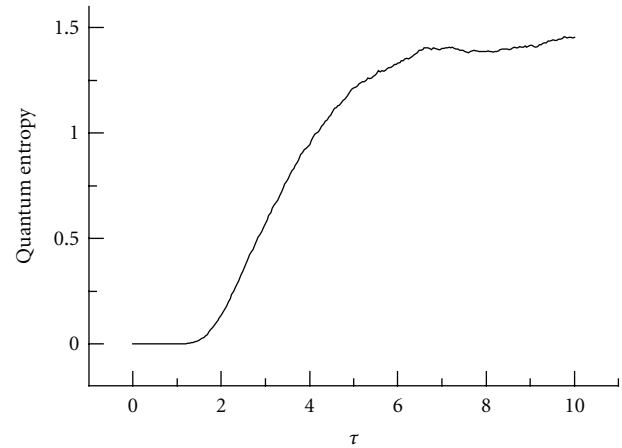

Figure 17: Dynamics of the quantum entropy of the fundamental mode for the values of the system parameters $\varepsilon = 3$, $k = 0.1$.

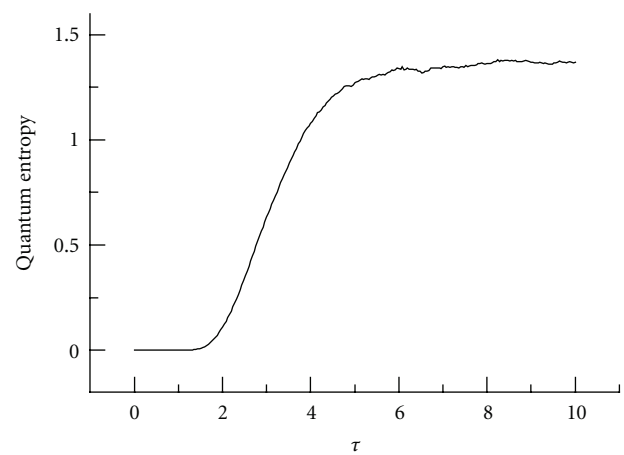

Figure 18: Dynamics of the quantum entropy of the third harmonic mode for the values of the system parameters $\varepsilon = 3$, $k = 0.1$.

and of an arbitrarily chosen quantum trajectory of the third harmonic mode (curve b). In the region of short interaction times ($\tau < 2$), the dynamics of the mean number of photons coincides with the dynamics of an arbitrary quantum trajectory. Later, the number of photons of an arbitrary quantum trajectory fluctuates around the mean number of photons of the mode.

Shown in Figures 17 and 18 is the dynamics of the quantum entropy of the fundamental and third harmonic modes, respectively. In the region of short interaction times ($\tau < 2$) the values of quantum entropy of the modes are equal to zero. The latter observation shows that the ensemble of the quantum trajectories of the system consists of a single element in this region of interaction time, which explains the coincidence of the dynamics of the mean number of photons with the dynamics of the number of photons of an arbitrarily chosen quantum trajectory of the corresponding modes. In the region of long interaction time, the dynamics of the quantum entropies of the modes changes to a stationary behavior. In the region of long interaction time, in contrast to the case of strong coupling of the modes shown in Figures 3 and 4, the stationary values of the quantum entropies of the modes are equal.

Shown in Figures 19 and 20 is the dynamics of the Wigner functions of the fundamental and third harmonic modes, respectively. At time of interaction $\tau \approx 2$ the fundamental mode changes from vacuum state into a pure squeezed state. The quantum entropy of this state is equal to zero. After that, the squeezed state decays, and in the region of long interaction time, ($\tau = 10$), the fundamental mode localizes to an unstable state, the Wigner function of which is shown in Figure 19(b). The Wigner function represents a two-component state with coupling of the components of

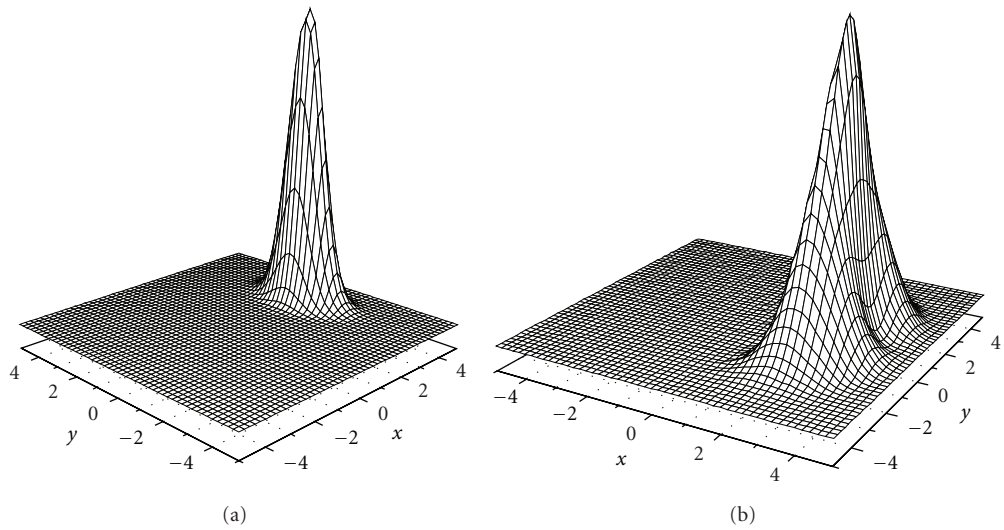

Figure 19: Dynamics of the Wigner function of the state of the fundamental mode for the values of the system parameters $\varepsilon = 3$, $k = 0.1$. Figures (a) and (b) illustrate the Wigner function at times of interaction of the modes $\tau = 2$, $\tau = 10$, respectively.

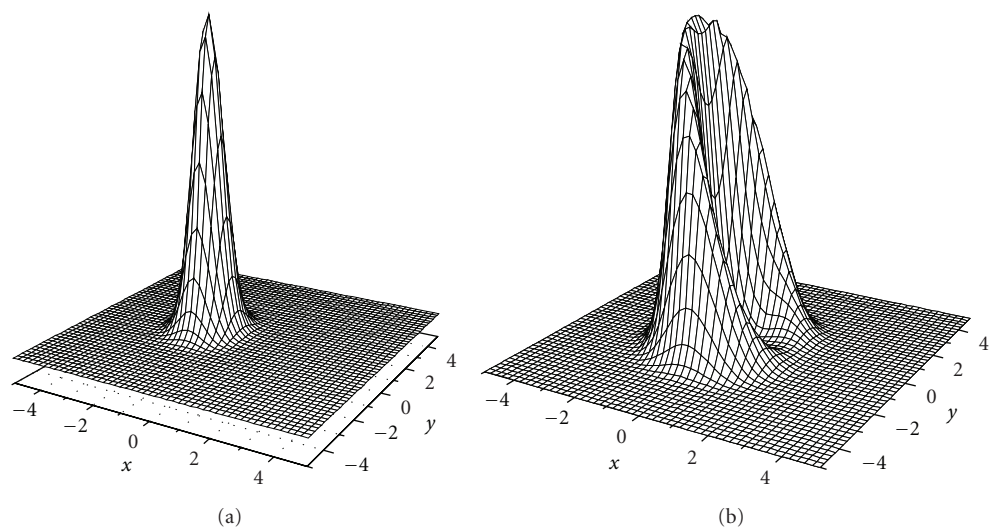

Figure 20: Dynamics of the Wigner function of the state of the third harmonic mode for the values of the system parameters $\varepsilon = 3$, $k = 0.1$. Figures (a) and (b) illustrate the Wigner function at times of interaction of the modes $\tau = 2$ and $\tau = 10$, respectively.

the state. The quantum entropy of this state approximately equals 1.4. Near time of interaction $\tau = 2$, the mode of the third harmonic localizes to a pure coherent state (see Figure 20(a)) (the quantum entropy is equal to zero) from the initial vacuum state. After that the coherent state of the mode decays, and in the region of long interaction time ($\tau = 10$), the mode localizes to a stationary unstable state, the Wigner function of which is shown in Figure 20(b).

In this case the Wigner function has a two-component structure with coupling of the components of the state. This observation contrasts with the case of strong coupling of the modes and strong perturbation of the fundamental mode, where the Wigner function has cylindrical form (see Figure 6(e)) in the region of long interaction times and where the behaviour of the system is unstable.

Acknowledgments

The authors are grateful to A. Chirkin, A. Melikyan, and R. Kostanyan for helpful discussions and to N. Aramian and O. Gevorgyan for technical assistance.

References

[1] P. D. Drummond, K. J. McNeil, and D. F. Walls, "Non-equilibrium transitions in sub/second harmonic generation," *Optica Acta: International Journal of Optics*, vol. 27, no. 3, pp. 321–335, 1980.

[2] P. D. Drummond, K. J. McNeil, and D. F. Walls, "Non-equilibrium transitions in sub/second harmonic generation," *Optica Acta: International Journal of Optics*, vol. 28, no. 2, pp. 211–225, 1981.

[3] S. T. Gevorkyan, G. Y. Kryuchkyan, and K. V. Kheruntsyan, "Noise, instability and squeezing in third harmonic generation," *Optics Communications*, vol. 134, no. 1–6, pp. 440–446, 1997.

[4] M. Dörfle and A. Schenzle, "Bifurcations and the positive P-representation," *Zeitschrift für Physik B*, vol. 65, no. 1, pp. 113–131, 1986.

[5] C. M. Savage, "Oscillations and quantized second-harmonic generation," *Physical Review A*, vol. 37, no. 1, pp. 158–162, 1988.

[6] R. Schack and A. Schenzle, "Moment hierarchies and cumulants in quantum optics," *Physical Review A*, vol. 41, no. 7, pp. 3847–3852, 1990.

[7] P. Goetsch and R. Graham, "Quantum trajectories for nonlinear optical processes," *Annalen der Physik*, vol. 505, no. 8, pp. 706–719, 1993.

[8] S. T. Gevorkyan and W. H. Maloyan, "Critical phenomena in the temporal behaviour of phase in second harmonic generation," *Journal of Modern Optics*, vol. 44, no. 8, pp. 1443–1452, 1997.

[9] S. T. Gevorkyan, "Bifurcation and quantum delocalized states in second-harmonic generation," *Physical Review A*, vol. 62, no. 1, Article ID 013813, 7 pages, 2000.

[10] S. T. Gevorkyan, G. Y. Kryuchkyan, and N. T. Muradyan, "Quantum fluctuations in unstable dissipative systems," *Physical Review A*, vol. 61, no. 4, Article ID 043805, 10 pages, 2000.

[11] S. T. Gevorkyan, "Quantum superposition states in third-harmonic generation," *Physical Review A*, vol. 58, no. 6, pp. 4862–4867, 1998.

[12] S. T. Gevorkyan and M. S. Gevorkyan, "Fluctuations in the number of photons above the bifurcation point in the process of third harmonic generation," *Optics and Spectroscopy*, vol. 107, no. 1, pp. 122–128, 2009.

[13] L. Gilles, B. M. Garraway, and P. L. Knight, "Generation of nonclassical light by dissipative two-photon processes," *Physical Review A*, vol. 49, no. 4, pp. 2785–2799, 1994.

[14] K. Mølmer, Y. Castin, and J. Dalibard, "Monte Carlo wave-function method in quantum optics," *Journal of the Optical Society of America B*, vol. 10, no. 3, pp. 524–538, 1993.